Reversing Along a Curved Path by an Autonomous Truck–Semitrailer Combination

Levente Mihályi[1] and Dénes Takács[1]

Department of Applied Mechanics, Faculty of Mechanical Engineering,
Budapest University of Technology and Economics, Műegyetem rkp. 3.,
H-1111 Budapest, Hungary.
mihalyi@mm.bme.hu

Abstract. In this paper, the stability analysis of the reverse motion along a circular path is presented for the truck–semitrailer combination. The dynamics of the low-speed manoeuvre are investigated with the single track kinematic model, supplemented with the model of the steering system. The time delay emerging in the control loop is also considered. The actuation is achieved by the steering of the truck, for which a linear feedback controller is designed to ensure the stability of the motion, meanwhile, a geometry-based feedforward steering angle is also used to force the system to the desired path. Linear stability charts are calculated in order to properly tune the control gains of the feedback controller with respect to the curvature of the path.

Keywords: autonomous vehicle, truck–semitrailer, reversing, time delay, path-following

1 Introduction

Self-driving vehicles could help society in several ways: they may make transportation safer, may reduce fuel consumption, and may improve the comfort of passengers. In freight transportation, self-driving of trucks, which are equipped with at least one trailer, generates different problems compared to a single passenger car [1].

One magnificent task to solve with automated delivery vehicles could be handling long convoys with only one human driver in the front, significantly reducing air resistance for the entire convoy. On the other hand, self-driving features make possible and improve the realization of complicated maneuvers. For example, the slow-speed reversing motion is a challenging task for drivers due to the instability of this motion that can also lead to the so-called Jackknifing phenomenon [2] in the worst case. However, reversing is unavoidable even for vehicle systems equipped with more than one trailer [3–5]. In this topic, some driver assistance systems (DAS) are already available, even with human input, where the controller helps the driver to follow the desired path and stabilizes the motion [6]. These features could be useful mostly in the loading bays. Docking maneuver in the loading bay is one of the most difficult and time-consuming tasks

of a truck driver [7]. Therefore, installing a fully autonomous control system in the area could save time and money for the companies and reduce accidents during loading.

In this paper, we analyze the dynamics of the truck–semitrailer combination, which is the most common vehicle type for freight transport worldwide. Based on previous research, a single track kinematic model supplemented by the steering dynamics is presented. The relevance of considering the steering mechanism is shown as well. Applying a coordinate transformation on the equations of motion enables the examination of the general path-following control; however, at this point, the curvature of the path is assumed to be a constant value. The purpose of this paper is to apply a simple linear feedback control for stabilizing the reverse motion of the truck–semitrailer along a circular path and to observe the effect of the curvature on stability. As a major contribution, the effect of time delay in the control loop is also considered in order to make the results more realistic. Then, linear stability charts are constructed from which the control gains can be tuned according to the desired curvature values. This method is also helpful in path designing for different trailer configurations. Nonlinear simulations show the performance of the controller designed by means of the stability analysis.

2 Mechanical model

The single track kinematic model of the truck–semitrailer is shown in Fig. 1. The vehicle system is modeled by two rods, neglecting the lateral extent of the vehicle. These rods represent the chassis of the truck and the semitrailer, which are connected at the kingpin K. The rigid wheels of the single track vehicle model are located at points F and R for the truck and at point T for the semitrailer. The wheelbase is referred to l, the distance of the kingpin and the rear axle of the truck is denoted by a; l_2 is the distance between the kingpin and the axle of the semitrailer, see Fig. 1. The steering angle δ refers to the only actuated variable of the vehicle system, x_{R}, y_{R}, ψ and φ are used to express the position of the truck, and the trailer. Namely, x_{R} and y_{R} are the coordinates of point R, the absolute yaw angle of the truck is denoted by ψ, while the yaw angle of the trailer relative to the truck's longitudinal axis is φ.

2.1 Equations of motion

The equations of motion are rooted in the kinematic constraints of the rolling rigid wheels, which ensure that the velocity vector of each axle at F, R, and T points are parallel to the proper wheel plane, i.e., perpendicular to the axle itself. Another kinematic constraint is also considered, namely, the longitudinal speed of the truck's rear axle is kept at the constant value V. After rearranging

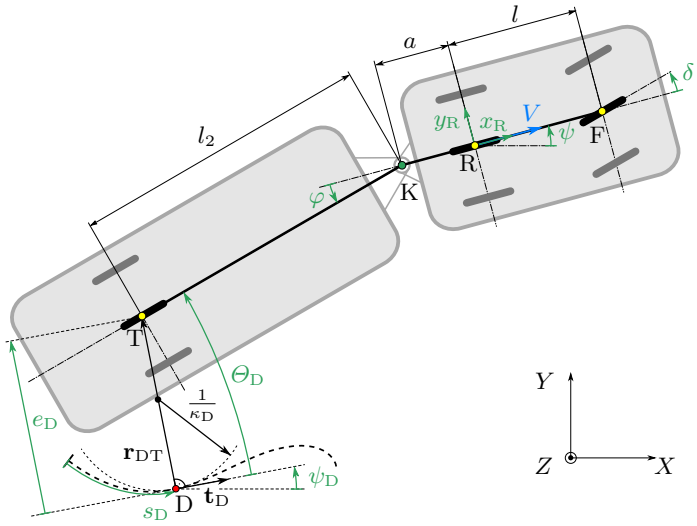

Fig. 1: Mechanical model of the truck–semitrailer

the constraining equations, they read

$$\begin{aligned} \dot{x}_\mathrm{R} = V\cos\psi, \quad \dot{y}_\mathrm{R} = V\sin\psi, \quad \dot{\psi} = \frac{V}{l}\tan\delta, \\ \dot{\varphi} = -\frac{V}{ll_2}\big(l\sin\varphi + (l_2 + a\cos\varphi_2)\tan\delta\big). \end{aligned} \tag{1}$$

Besides the higher-level controller, which will be introduced in Section 3, there is a lower-level controller in the model for operating the steering of the vehicle. Thus, the dynamics of the steering system is described by

$$\dot{\delta} = \omega, \quad \dot{\omega} = -p(\delta - \delta_\mathrm{des}) - d\omega. \tag{2}$$

Here, δ_des denotes the desired steering angle, which is determined by the higher-level controller. The steering rate is denoted by ω, i.e., (2) refers to the PD-controlled one degree-of-freedom steering mechanism. The notations p and d are the proportional and the derivative gains of the lower-level controller. An alternative modeling approach is the use of direct assignment of the steering angle, however, taking the dynamics of the steering mechanism into account results quantitatively different stability charts, as it will be shown in Subsection 4.2.

2.2 Path-following

In order to obtain the governing equations for investigating the path-following control, there are two more steps left. The most obvious point of the vehicle system to be prescribed to follow the path in reverse motion is the axle of the trailer

(T). So, first, the position of the trailer's axle (point T) in the (X, Y) ground-fixed coordinate system has to be determined as a function of the generalized coordinates x_R, y_R, ψ and φ. On the other hand, a coordinate transformation is needed to the path-reference frame (see [8] for details), where the system is described by the state vector:

$$\mathbf{x} = \left[s_\mathrm{D}\ e_\mathrm{D}\ \Theta_\mathrm{D}\ \psi\ \varphi\ \delta\ \omega \right]^\mathrm{T}, \tag{3}$$

where the first three components refer to the path-following problem (see Fig. 1). The index D refers to the closest point to T along the path, s_D is the arclength along the path, e_D (lateral deviation) is the distance between the points T and D, and $\Theta_\mathrm{D} = \psi + \varphi - \psi_\mathrm{D}$ is the angle of the trailer relative to the path. The curvature of the path at point D is marked with κ_D. In general, the curvature $\kappa_\mathrm{D}(s_\mathrm{D})$ can depend on the arclength, but in this study, it is assumed to be constant, which implies a circular path.

Finally, the governing equations can be obtained as follows

$$\begin{aligned} \dot{s}_\mathrm{D} &= \frac{V}{1-\kappa_\mathrm{D} e_\mathrm{D}} \left(\cos\left(\Theta_\mathrm{D} - \varphi\right) + \frac{a}{l} \tan\delta \sin\left(\Theta_\mathrm{D} - \varphi\right) \right) \\ &\quad - \frac{V}{1-\kappa_\mathrm{D} e_\mathrm{D}} \left(\sin\varphi + \frac{a}{l} \cos\varphi \tan\delta \right) \sin\Theta_\mathrm{D}\,, \end{aligned} \tag{4}$$

$$\begin{aligned} \dot{e}_\mathrm{D} &= V \left(\sin\left(\Theta_\mathrm{D} - \varphi\right) - \frac{a}{l} \tan\delta \cos\left(\Theta_\mathrm{D} - \varphi\right) \right) \\ &\quad + V \left(\sin\varphi + \frac{a}{l} \cos\varphi \tan\delta \right) \cos\Theta_\mathrm{D}\,, \end{aligned} \tag{5}$$

$$\dot{\Theta}_\mathrm{D} = \dot{\psi} + \dot{\varphi} - \kappa_\mathrm{D} \dot{s}_\mathrm{D}, \tag{6}$$

$$\dot{\psi} = \frac{V}{l} \tan\delta\,, \tag{7}$$

$$\dot{\varphi} = -\frac{V}{l l_2} \left(l \sin\varphi + \left(l_2 + a\cos\varphi\right) \tan\delta \right), \tag{8}$$

$$\dot{\delta} = \omega, \tag{9}$$

$$\dot{\omega} = -p\delta - d\omega + p\delta_\mathrm{des}\,. \tag{10}$$

It is worth mentioning that the right hand side of Eq. (6) can be substituted by (4), (7) and (8), which are not accomplished here to reduce the complexity of the formulas. However, using the state vector (3), Eqs. (4)–(10) can be given in the affine form

$$\dot{\mathbf{x}} = \mathbf{f}(\mathbf{x}) + \mathbf{g}(\mathbf{x})\mathbf{u}\,, \tag{11}$$

where the input $\mathbf{u}$ refers to the desired steering angle δ_des.

3 Control algorithm

In order to keep the system on the desired path, a higher-level controller is introduced that determines the desired steering angle (the input of the controlled

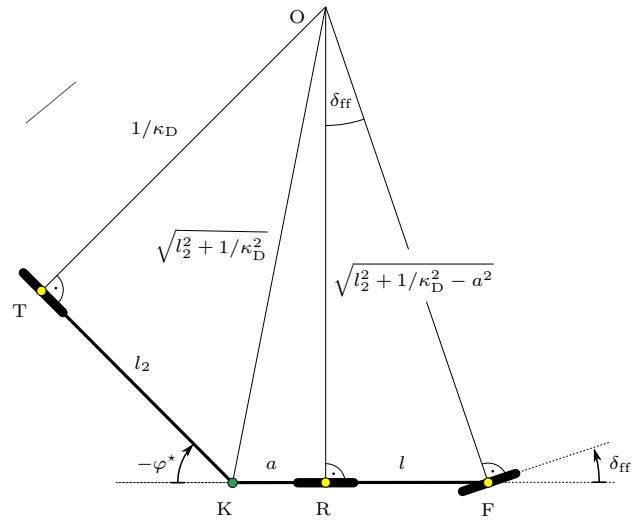

Fig. 2: Geometry aspect of feedforward steering angle δ_{ff} and equilibria of the relative yaw angle $\varphi^\star$ of the trailer

vehicle system). Namely:

$$\delta_{\mathrm{des}}(t) = \delta_{\mathrm{ff}} + \delta_{\mathrm{fb}}(t), \tag{12}$$

where the curvature-dependent feedforward term is denoted by δ_{ff}, while the feedback term δ_{fb} is based on the state variables.

The value of the feedforward steering angle can be calculated by solving the equations of motion Eqs. (6) and (8) for the steady state solution (circular motion). This solution can also be determined based on geometrical approach shown in Fig. 2. Starting from the curvature, the feedforward term can be given as

$$\delta_{\mathrm{ff}} = \arctan \frac{l}{\sqrt{l_2^2 + 1/\kappa_{\mathrm{D}}^2 - a^2}}. \tag{13}$$

To ensure the stability of the reverse motion, the linear feedback δ_{fb} is designed with three proportional terms:

$$\delta_{\mathrm{fb}}(t) = -P_e e_{\mathrm{D}}(t-\tau) - P_\Theta \Theta_{\mathrm{D}}(t-\tau) - P_\varphi \left(\varphi(t-\tau) - \varphi^\star\right), \tag{14}$$

where τ is the time delay that is primarily rooted in sensor data processing and control algorithm execution that can be relevant even in the case of autonomous vehicles. The angle $\varphi^\star$ in Eq. (14) is the yaw angle of the trailer relative to the truck in steady state condition, which can be calculated based on the geometric approach (see Fig. 2):

$$\varphi^\star = -\left(\pi - \arctan \frac{1}{\kappa_{\mathrm{D}} l_2} - \arccos \frac{a}{\sqrt{l_2^2 + 1/\kappa_{\mathrm{D}}^2}}\right). \tag{15}$$

4 Stability analysis

The main results of our analysis are manifested in stability charts, by which the effects of different parameters on the linear stability can be investigated. Probably the most critical parameters are the gains of the feedback controller while assuming a vehicle combination with fixed geometry. Beyond the effect of the control gains, our research also focuses on the effect of path curvature.

4.1 Linearization

This paper presents a linear stability analysis of the reverse circular motion. Accordingly, the linearized form of the governing equations (4)–(10) is needed. More precisely, the equation related to the arclength Eq. (4) can be eliminated because the stability of the motion is independent of this variable in the linear sense, so as Eq. (7). Hence, the steady state solution, around which the linearization is accomplished, reads

$$\mathbf{x}^\star = \left[e_\mathrm{D}^\star \; \Theta_\mathrm{D}^\star \; \varphi^\star \; \delta^\star \; \omega^\star\right]^\mathrm{T} = \left[0 \; 0 \; \varphi^\star \; \delta_\mathrm{ff} \; 0\right]^\mathrm{T}. \tag{16}$$

As introducing a perturbation $\tilde{\mathbf{x}}$ and $\tilde{\mathbf{u}}$, so that

$$\mathbf{x}(t) = \mathbf{x}^\star + \tilde{\mathbf{x}}(t), \quad \mathbf{u}(t) = \mathbf{u}^\star + \tilde{\mathbf{u}}(t), \tag{17}$$

let us obtain the linear state space representation in the form of

$$\dot{\tilde{\mathbf{x}}}(t) = \mathbf{A}\,\tilde{\mathbf{x}}(t) + \mathbf{B}\,\tilde{\mathbf{u}}(t-\tau). \tag{18}$$

In the Jacobian linearization above, $\mathbf{A}$ is the system matrix, $\mathbf{B}$ is the input matrix (in this case a vector), and $\mathbf{u} = \left[\delta_\mathrm{des}\right]$ indicates the control input vector (in this case a scalar). These matrices can be determined by

$$\mathbf{A} = \left.\frac{\partial \mathbf{f}}{\partial \mathbf{x}}\right|_{\mathbf{x}^\star} \text{ and } \quad \mathbf{B} = \mathbf{g}(\mathbf{x}^\star), \tag{19}$$

which reads as follows

$$\mathbf{A} = \begin{bmatrix} 0 & v & 0 & 0 & 0 \\ -v\kappa_\mathrm{D}^2 & 0 & V\kappa_\mathrm{D}\left(\sin\varphi^\star + \dfrac{a}{l}\tan\delta_\mathrm{ff}\cos\varphi^\star\right) - \dfrac{v}{l_2} & r\left(\cos\varphi^\star - \kappa_\mathrm{D} l_2 \sin\varphi^\star\right) & 0 \\ 0 & 0 & -\dfrac{v}{l_2} & r\left(\cos\varphi^\star + \dfrac{l_2}{a}\right) & 0 \\ 0 & 0 & 0 & 0 & 1 \\ 0 & 0 & 0 & -p & -d \end{bmatrix} \tag{20}$$

$$\mathbf{B} = \left[0 \; 0 \; 0 \; 0 \; p\right]^\mathrm{T}, \tag{21}$$

where:

$$v := \frac{V}{l}\left(l\cos\varphi^{\star} - a\sin\varphi^{\star}\tan\delta_{\mathrm{ff}}\right), \tag{22}$$

$$r := -\frac{Va}{ll_2\cos^2\delta_{\mathrm{ff}}}. \tag{23}$$

Based on the system matrix $\mathbf{A}$ and the control input vector $\mathbf{B}$, the controllability of the system can be checked, which condition is fulfilled for our system.

4.2 Effect of curvature

In this subsection, the semi-discretization method [9] is applied to investigate the stability of the controlled reverse motion. Stability charts are generated in the $P_\Theta - P_\varphi$ plane, meanwhile, we fixed the control gain of the lateral error to $P_e = -5$ rad/m. In order to analyze the effect of curvature on stability, the time delay is also fixed, namely, we consider $\tau = 0.1$ s. All the other required geometrical and control parameters are listed in Table 1.

In Fig. 3 (a), linearly stable control gain domains are depicted by blue colors. Different shades of blue refer to different curvature values, as labeled on the chart. Cyan dots denote the most stable gain configuration for the different curvatures, i.e., the smallest real part of the rightmost eigenvalue is ensured at these points. On the one hand, as it is shown by the figure, the reverse circular motion can be stabilized even in the case of a path with relatively small turning radius (reciprocal of curvature) if the control gains are correctly set. On the other hand, tuning the control gains is a crucial task to achieve stability for very different path curvatures. For example, even the most stable gain setup for $\kappa_{\mathrm{D}} = 0.1\,\mathrm{m}^{-1}$ is located outside the stable domain for $\kappa_{\mathrm{D}} = 0.2\,\mathrm{m}^{-1}$.

A comparison with the assigned steering angle case is shown in panel (b), where the curvature values are the same as in panel (a). As shown, the assigned steering angle approach results unrealistically large stable areas (bordered by dashed lines), which demonstrates the importance of considering the steering mechanism. However, the most stable gain setups of the assigned steering angle case (marked with cyan crosses) are also located inside of the stable domain of the stricter, steering mechanism case.

Table 1: Vehicle parameters applied in our analysis

Parameter	Value	Unit
V	-3	m/s
a	-0.8	m
l	3.5	m
l_2	10	m
p	300	$1/\mathrm{s}^2$
d	34.6	1/s

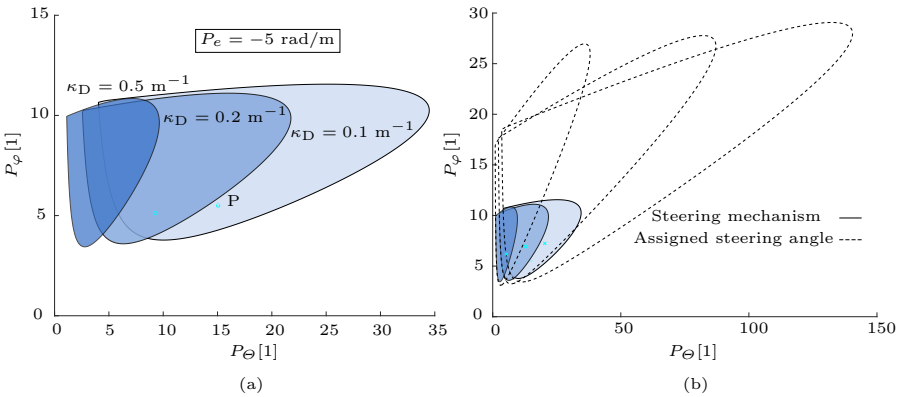

Fig. 3: (a) Stability charts for demonstrating the effect of curvature of the desired path κ_D on stability ($\tau = 0.1$ s). (b) Comparison of the steering mechanism and the assigned steering angle cases.

5 Simulation

Simulations are carried out in order to verify the results. Time series graphs are acquired by solving the nonlinear equations of motion Eq. (4)–(10), complemented with the derivative of the truck's rear axle position x_R and y_R in order to track the trajectory of the truck–semitrailer in the (X, Y) coordinate system.

The most stable gain configuration in the case of $\kappa_D = 0.1\,\mathrm{m}^{-1}$ is considered (see parameter point P in Fig. 3), i.e., $P_e = -5$ rad/m, $P_\Theta = 15$ and $P_\varphi = 5.5$. Simulations are done both for $0.1\,\mathrm{m}^{-1}$ and $0.2\,\mathrm{m}^{-1}$ curvature values in Figs. 4 and 5, respectively. Initially, the truck–semitrailer combination is set in a position and orientation that corresponds to $e_D = 0.1$ m, $\Theta_D = 0$, $\varphi = \varphi^\star$, $\delta = \delta_{ff}$, $\omega = 0$, $x_R = 0$, $y_R = 0$ and $\psi = 0$. The initial and final positions and orientations are illustrated by black and red colors, respectively. The outer and inner blue curves are the path of the truck's rear axle (point R) and the trailer's axle (point T), respectively. Furthermore, the desired circular path of the trailer's axle is denoted by magenta dashed line, which infers an insignificant difference between the desired and the realized path of the trailer's axle (point T). Note that an initial perturbation was applied in the lateral position.

Time histories of state variables can be seen on the left panels of Figs. 4 and 5. It can be seen that while the path following is stable for the smaller curvature, the simulation ends with jackknifing for the larger curvature, i.e., the path following is unstable. This proves the importance of proper gain tuning; thus, different gains must be set according to the curvature of the path. On the right panels of Figs. 4 and 5, trajectories are plotted to visualize the stable and unstable nature of the motion.

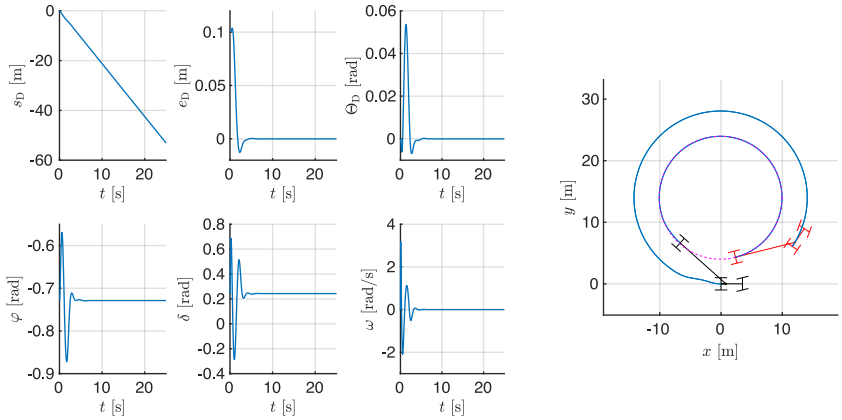

Fig. 4: Simulation results of the stable motion ($\kappa_D = 0.1$)

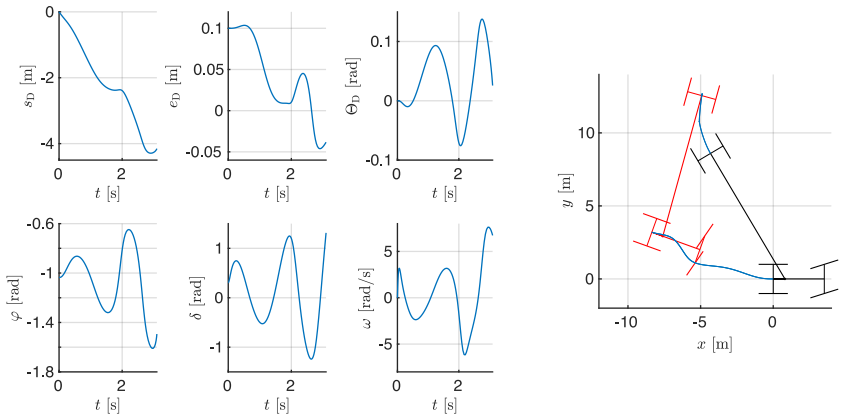

Fig. 5: Simulation results of the unstable motion ($\kappa_D = 0.2$) with the jackknifing phenomenon on the right

6 Conclusion

It was introduced that the naturally unstable reverse motion of a truck–semitrailer can be stabilized along a circular path even in the presence of significant time delay. A control algorithm was designed to realize the stabilization and keep the vehicle system on the desired and prescribed path. Moreover, the kinematic model was supplemented with the steering dynamics. It was shown that the steering dynamics has a relevant role in the proper tuning of the controller. It has been proven that the path-following problem can be solved for constant curvature, but the control gains must be tuned according to the curvature value. The results were verified by nonlinear simulations, which also helped to visualize the stable and unstable nature of the motion, as well as to observe the jackknifing phenomenon.

Detailed parameter analysis can be investigated in the future. The value of the critical time delay, for which the reverse motion cannot be stabilized, can also be calculated as a function of the reversing speed. Moreover, some scenarios of exact commercial trailer types should be set. These steps would allow us to validate the results by experimental tests on small-scale equipment or even in a real environment. Another helpful feature could be extending the path-following control to a general case when the curvature varies along the prescribed path (e.g., along a clothoid). The varying curvature probably causes the need for adaptive control gain tuning.

Acknowledgement

The research reported in this paper was partly supported by the János Bolyai Research Scholarship of the Hungarian Academy of Sciences and by the National Research, Development and Innovation Office under grant no. NKFI-128422 and under grant no. 2020-1.2.4- TÉT-IPARI-2021-00012.

References

1. Roh J, Chung W. Reversing Control of a Car with a Trailer Using the Driver Assistance System. International Journal of Advanced Robotic Systems. 2011;8(2). doi:10.5772/10578
2. M. Hejase, J. Jing, J. M. Maroli, Y. Bin Salamah, L. Fiorentini and Ü. Özgüner, "Constrained Backward Path Tracking Control using a Plug-in Jackknife Prevention System for Autonomous Tractor-Trailers," 2018 21st International Conference on Intelligent Transportation Systems (ITSC), 2018, pp. 2012-2017, doi: 10.1109/ITSC.2018.8569262.
3. J. Cheng, Y. Zhang and Z. Wang, "Path tracking control for mobile robot with two trailers," Proceedings of the 32nd Chinese Control Conference, 2013, pp. 4337-4341.
4. Michałek, Maciej. (2014). A highly scalable path-following controller for N-trailers with off-axle hitching. Control Engineering Practice. 29. 61–73. 10.1016/j.conengprac.2014.04.001.
5. Chung, W., Park, M., Yoo, K. et al. Backward-motion control of a mobile robot with n passive off-hooked trailers. J Mech Sci Technol 25, 2895–2905 (2011). https://doi.org/10.1007/s12206-011-0909-7
6. Hafner, Mike and Pilutti, Tom. (2017). Control for Automated Trailer Backup. 10.4271/2017-01-0040.
7. A. C. Manav, I. Lazoglu and E. Aydemir, "Adaptive Path-Following Control for Autonomous Semi-Trailer Docking," in IEEE Transactions on Vehicular Technology, vol. 71, no. 1, pp. 69-85, Jan. 2022, doi: 10.1109/TVT.2021.3125131.
8. Qin, W.B., Zhang, Y., Takács, D. et al. Nonholonomic dynamics and control of road vehicles: moving toward automation. Nonlinear Dyn (2022). https://doi.org/10.1007/s11071-022-07761-4
9. Insperger, Tamás and Stépán, Gábor. (2011). Semi-discretization for time-delay systems—Stability and engineering applications. 10.1007/978-1-4614-0335-7.